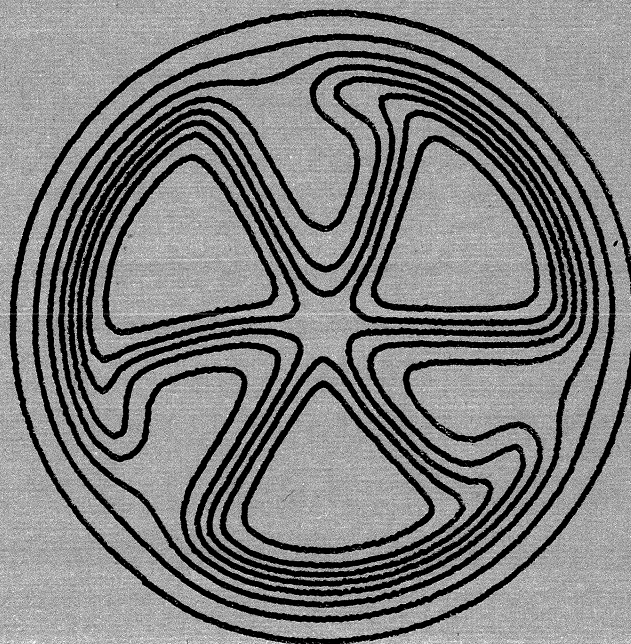


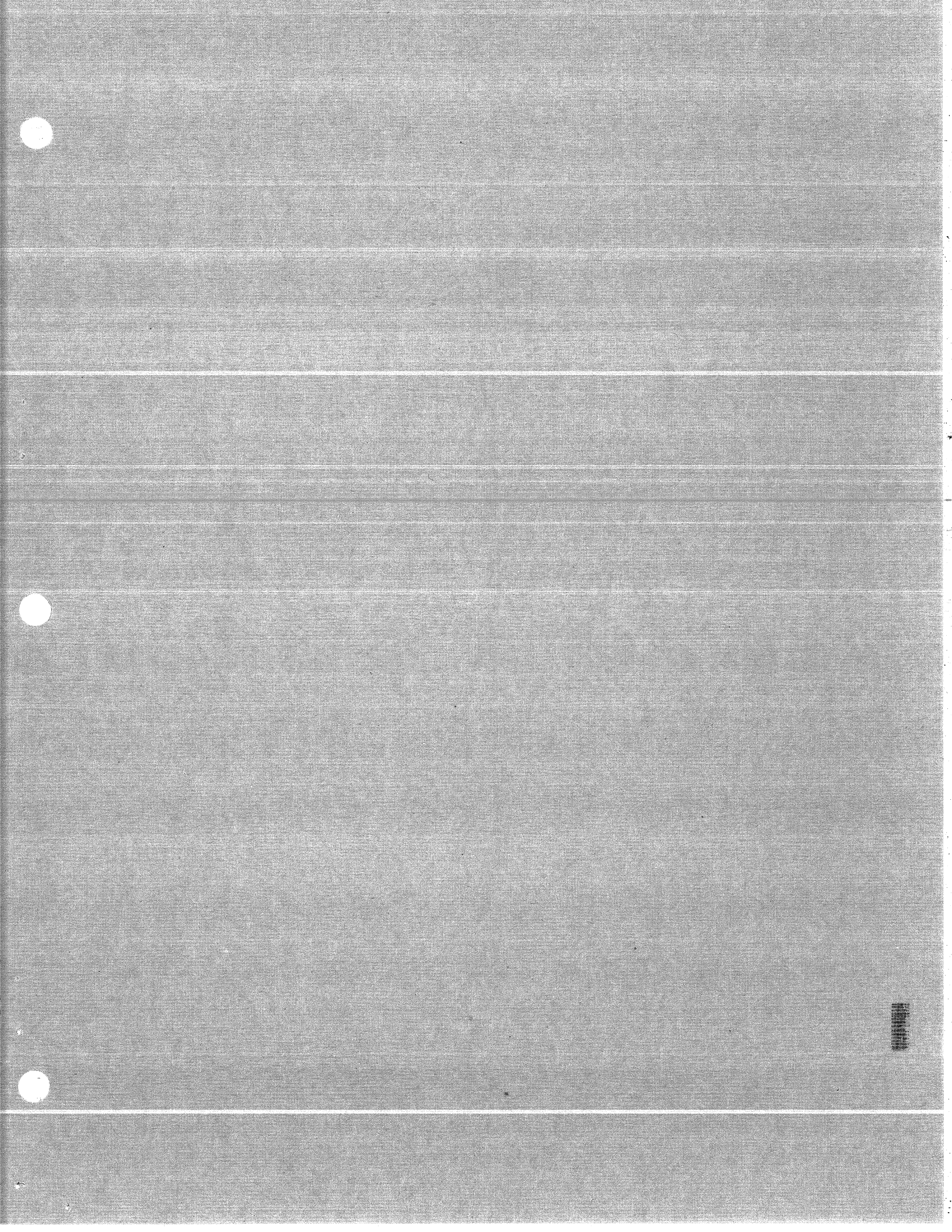
MICHIGAN STATE UNIVERSITY

CYCLOTRON LABORATORY

THE EXCITATION OF GIANT RESONANCES IN ELECTRON
AND PROTON SCATTERING

G.R. HAMMERSTEIN, H. McMANUS, A. MOALEM AND T.T.S. KUO





The Excitation of Giant Resonances in Electron
and Proton Scattering[†]

G.R. Hammerstein, H. McManus and A. Moalem
Cyclotron Laboratory and Physics Department
Michigan State University, East Lansing, Mi. 48824

and

T.T.S. Kuo
State University of New York, Stony Brook, New York 11790

ABSTRACT

Microscopic model calculations are presented for various multipole states in ^{40}Ca . A resonance-like structure largely due to dipole and quadrupole states is predicted in the giant dipole region with qualitatively the same features observed in electron and proton scattering. The calculated cross-sections are in good agreement with those obtained from simple phenomenological collective models, and the available scattering experimental data.

[†]Supported in part by the National Science Foundation.

Inelastic scattering of electrons^{1,2} and hadrons^{3,4} on a wide range of nuclei shows strongly excited resonance-like structures in the low excitation region of the nuclear continuum. The giant dipole resonance (GDR), long known from photonuclear work, has proved inadequate by itself to explain the experimental results, and a giant isoscalar quadrupole resonance (GQR)^{3,5} or monopole resonance⁵ lying 2-3 Mev below the GDR has been proposed. In addition, other multipoles such as an octopole resonance have been suggested as an explanation for part of the observed strength. The resonance-like structures have been widely analyzed in terms of phenomenological collective models, which provide estimates of energy centroid and total available strength (through energy weighted sum rules) for the various multipoles but little information about possible fragmentation of this strength. It is of interest to see what is predicted by a completely microscopic model. A general approach to this problem has been given by Bertsch.⁶ In the present paper, however, we consider only a particular case--of a detailed RPA calculation for ^{40}Ca .⁷

Such calculations give an account of the fragmentation of the multipole strength among states formed by particle-hole excitations, but do not include the further fragmentation among multiparticle multi-hole states. To take this into account, we have simply attributed a spreading width, as in reference 6, to each RPA state.

We have considered states with $J^\pi(\Gamma)=0^+(0), 1^-(1), 2^+(0), 3^-(0)$ and $5^-(0,1)$ in the excitation energy region 10-25 Mev. While all of the E0, E1, and E5 strength is concentrated in one or two states, the calculations predict many 2^+ and 3^- states. Still,

considerable amount of E2 and E3 transition strength falls in the 10-25 MeV region.

The predictions of the RPA model are as follows:

- (1) Almost all of the isoscalar monopole strength lies in a single state at 14.0 MeV.
 - (2) The isovector non-spinflip dipole strength is concentrated in a state at 18.8 MeV, in good agreement with the location of the photonuclear GDR and the main structure of the low momentum transfer (e, e') spectrum. There is some isovector dipole strength in states at 16.5 and 21.3 MeV, the latter state being largely spinflip in character.
 - (3) The isoscalar quadrupole strength is contained in a group of states lying between 17 and 21 MeV, dominated by a state at 17.3 MeV.
 - (4) The isovector monopole and quadrupole strength is concentrated in the 23-34 MeV region. These states were not considered here.
 - (5) The 3^- strength is fragmented, although some isoscalar 3^- strength is located in the region of the monopole state.
- Table I summarizes the $B(EJ)$ values predicted for multipole states in various excitation energy regions.
- On this basis the excitation spectra and cross sections for inelastic scattering of electrons and protons for the 10-25 MeV region of excitation were calculated. Details of the scattering formalism used here are given in references 8 and 9. The (p, p') differential cross sections for incident energy 182 MeV were

calculated in distorted wave impulse approximation with a pseudopotential similar to that of ref. 9. For our purposes, the effects of the noncentral parts of the force could be included approximately in the central parts, of which only the isoscalar non-spinflip (V_{00}) and the isovector spinflip (V_{11}) components were important. Each was represented by the sum of a Yukawa force with $\mu = .843 \text{ fm}^{-1}$ and a zero range force: $V = Y_e^{-\mu r} / \mu r + Z \delta(r)$. The strengths, in an obvious notation, were $Y_{00} = 11.56 \text{ MeV}$, $Z_{00} = 113.4 \text{ MeV}$ and $Y_{11} = 5.39 \text{ MeV}$, $Z_{11} = 52.0 \text{ MeV}$. The electron scattering was calculated in Born approximation with a local wave number correction.⁸

The summed differential cross section for all states of a given J^π is very close to that of the strongest low lying collective states and to that obtained from phenomenological collective models. The present calculations, however, are absolute, with no adjustable parameters. They can be compared directly with the experimental differential cross sections extracted for large energy bites. Such comparisons are made in Figure 1 for (e, e') for the excitation energy range 10-25 MeV and in Figure 2 for the 182 MeV (p, p') data with energy bites 10-16 and 16-22 MeV. While the present results are in rather good accord with experiment, it is clear that the data do not preclude other conceivable combinations of multipoles.

To produce excitation spectra we folded the calculated cross section for a given state at a given momentum transfer with a Breit-Wigner shape. A spreading width $\Gamma = 4 \text{ MeV}$, corresponding to the observed width of the GDR¹⁰, was assumed for

states above 16 MeV, while for states below 16 MeV, i.e. those near neutron threshold, a width $\Gamma=2$ MeV was assumed. The only parameter in the calculation of strength distribution is the width Γ , which did not enter the calculations of the summed differential cross sections. With the spreading widths folded in, the predicted excitation curves lose the details of the RPA calculations. What is predicted for all probes is a broad structure in the 16-22 MeV region due primarily to dipole and quadrupole excitations, with a satellite structure at 14 MeV due mainly to monopole excitation with some octopole. We note here that a structure near 14 MeV, clearly seen in the (e,e') data of Reference 1, has also been observed recently in scattering of 60 MeV protons¹¹ and 115 MeV alphas.¹²

The predicted excitation spectra along with separate curves for the E0, E1, and E2 constituents are shown in figure 3 for (e,e') and Figure 4 for (p,p') at 182 MeV. Experimental data from References 1 and 3 are included for comparison. For the cases of Figures 3 and 4 the 3⁻ and 5⁻ states contribute a relatively flat background and are not shown separately. The centroid of the broad structure from 16 to 22 MeV depends mostly on the relative strength of the 2⁺ and 1⁻ states. At low momentum transfer the (e,e') spectrum is dominated by the 1⁻ states and the resonance-like peak is located near the photo-nuclear GDR position. With increasing momentum transfer the E1 strength dies away and the energy centroid shifts toward

the strong 2⁺ component at 17.3 MeV. In (p,p') at 182 MeV, where $V_{00} \sim 2V_{11}$, the E2 strength appears dominantly and the structure peaks near 17 MeV, except at very forward angles where the spin-flip dipole state at 21.3 MeV contributes strongly.

We conclude that the observation of a pronounced structure in the GDR region is well accounted for by nuclear shell theory and to a large extent its origin lies in the excitation of collective 2⁺ and 1⁻ states. It is an interesting question whether the secondary structure near 14 MeV is in fact due primarily to monopole excitation as predicted by the RPA calculations.

We are indebted to Prof. G. Bertsch for his comments on the manuscript.

REFERENCES

1. K. Itoh, M. Oyamada and Y. Torizuka, Phys. Rev. C2, 2181 (1970); K. Itoh, Y. Kawazoe, G. Takeda, Y. Torizuka and Y.M. Shin, to be published.
2. R. Pitthan and T. Walcher, Phys. Lett. 36B, 563(1971); F.R. Buskirk, H.D. Gref, R. Pitthan, H. Theissen, O. Titze and T. Walcher, Phys. Lett. 42B, 194(1972); S. Fukuda and Y. Torizuka, Phys. Rev. Lett. 29, 1109(1972); M. Nagao and Y. Torizuka, Phys. Rev. Lett. 30, 1071(1973); S. Klavansky, H.W. Kendall, A.K. Kerman and D. Isabelle, Phys. Rev. C7, 795(1972).
3. M.B. Lewis, Phys. Rev. Lett. 29, 1257(1972).
4. M.B. Lewis and F.E. Bertrand, Nucl. Phys. A196, 337(1972); M.B. Lewis, F.E. Bertrand and D.J. Horen, Phys. Rev. C8, 398(1973); M.B. Lewis, Phys. Rev. C7, 2041(1973); A. Moalem, W. Benenson and G.M. Crawley, Phys. Rev. Lett. 31, 482(1973).
5. G.R. Satchler, Nucl. Phys. A195, 1(1972); G.R. Satchler, Particles and Nuclei 5, 105(1973).
6. G.F. Bertsch, Phys. Rev. Lett. 31, 121(1973) and G.F. Bertsch and S.F. Tsai, to be published.
7. Extension of the calculations in J. Blomqvist and T.T.S. Kuo, Phys. Lett. 29B, 544(1969).
8. G.R. Hammerstein, R.H. Howell, and F. Petrovich, Nucl. Phys. A213, 45(1973).
9. R.M. Haybron and H. McManus, Phys. Rev. 140B, 638(1965).
10. M. Bezic, D. Jamnik, G. Kernel, J. Krafnik and J. Snajder, Nucl. Phys. A117, 124(1968).
11. D.C. Kocher, F.E. Bertrand, E.F. Gross, R.S. Lord and E. Newman, Bull. Am. Phys. Soc. 18, 1386(1973); and F.E. Bertrand, private communication.
12. J.M. Moss, D.H. Youngblood, C.M. Rozsa, L. Rutledge and J.D. Bronson, Bull. Am. Phys. Soc. 19, 110(1973).

Table I: Values of $B(EJ)$ for multipole states in the continuum region in ^{40}Ca .

J^π, T	$0^+, 0$	$1^-, 1$	$2^+, 0$	$3^-, 0$	$3^-, 1$	$5^-, 0$	$5^-, 1$
10-16	7.4	-0	-0	2.7	5.5	3.1	3.3
16-22	1.9	5.2	12.7	0.5	4.3	4.6	6.6
22-25	0.6	-0	0.9	-0	-0	-0	-0

The numbers listed are the radial matrix element $\langle r^2 \rangle_{if}$ for the monopole states and the electromagnetic transition rates in single particle units for the other multipoles.

FIGURE CAPTIONS

- Figure 1. Inelastic electron scattering form factors for the giant resonance region of ^{40}Ca . The solid curve is the sum due to all states in the region 10-25 MeV. Separate contributions of various multipoles are shown as dashed curves. The data points are taken from Ref. 1.
- Figure 2. Angular distributions for (p,p') at 182 MeV. The data points are from Ref. 3. The upper curve gives the sum for all states in the excitation region 16-22 MeV (mostly dipole and quadrupole). The lower solid curve is the sum of all states in the 10-16 MeV region (mostly monopole), with the contribution from octopole alone shown as the dashed curve.
- Figure 3. Excitation curves for multipole states in the reaction $^{40}\text{Ca}(e,e')^{40}\text{Ca}$. The solid curve is the sum due to all states in the region 10-25 MeV (see text). The $E0(T=0)$, $E1(T=1)$, and $E2(T=0)$ constituents are shown as dotted, dashed-dotted, and dashed curves respectively. The shaded area represents an experimental spectrum taken from Ref. 1.
- Figure 4. Excitation curves for multipole states in the $^{40}\text{Ca}(p,p')^{40}\text{Ca}$ reaction. The solid curve is due to all states in the region 10-25 MeV (see text). The $E0(T=0)$, $E1(T=1)$, and $E2(T=0)$ constituents are shown as dotted, dashed-dotted, and dashed curves respectively. The data points are those of Ref. 3.

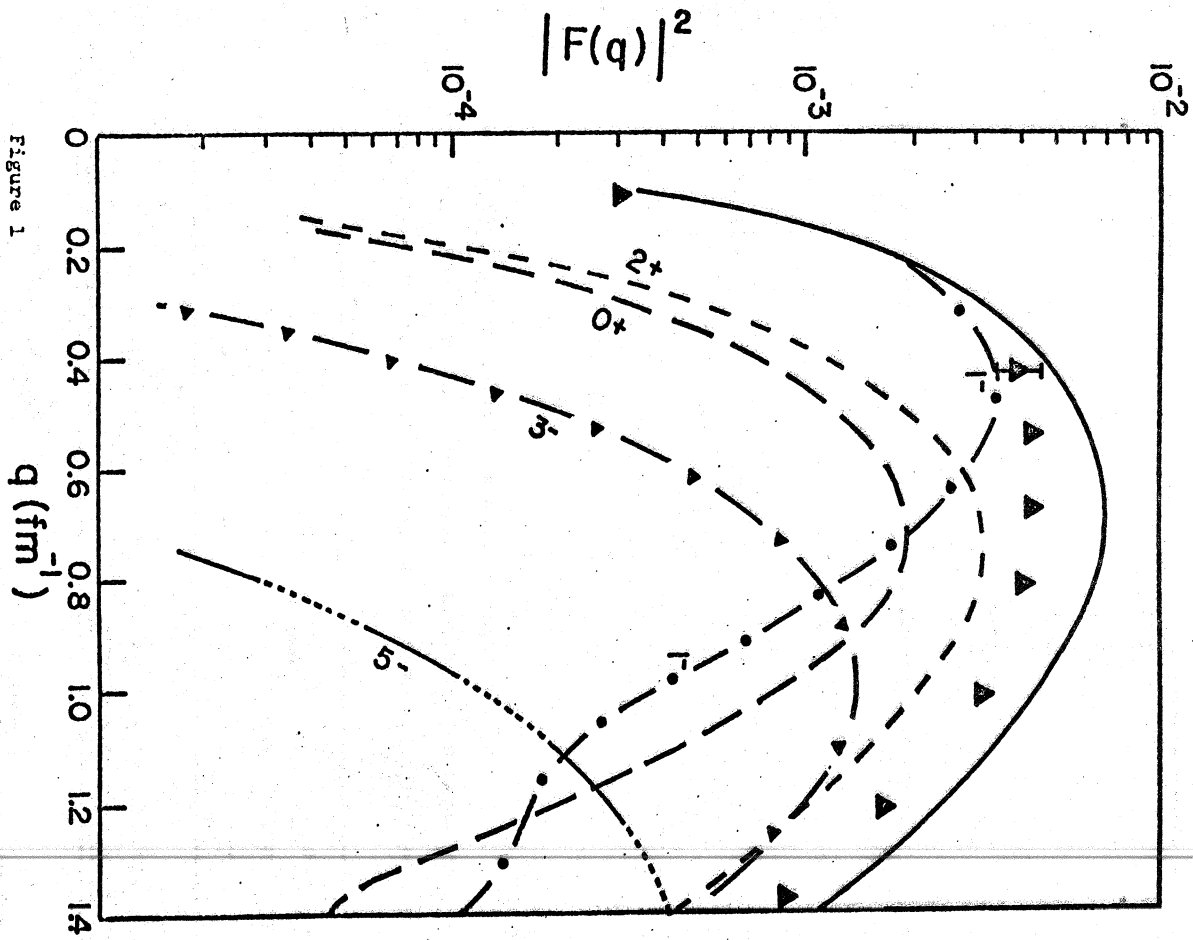


Figure 1

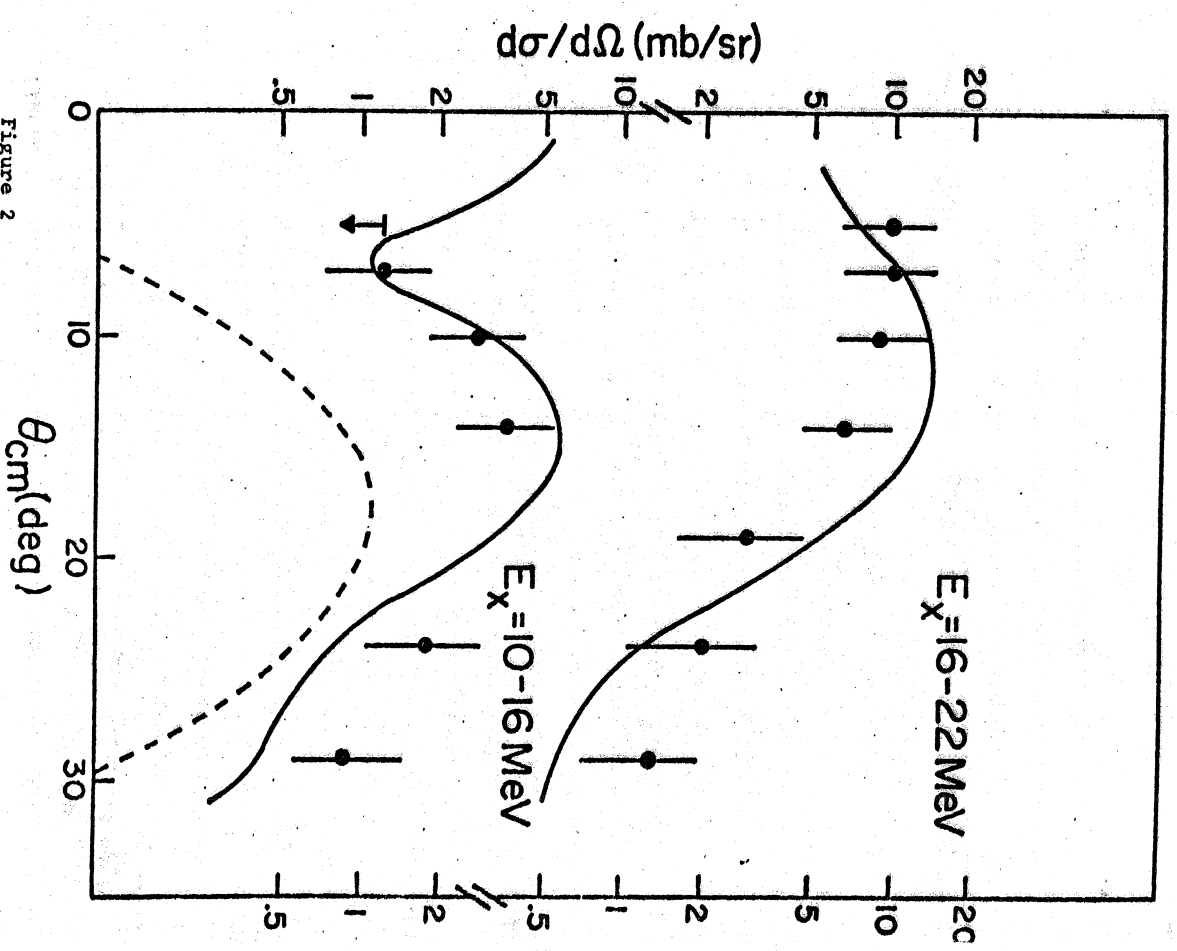


Figure 2

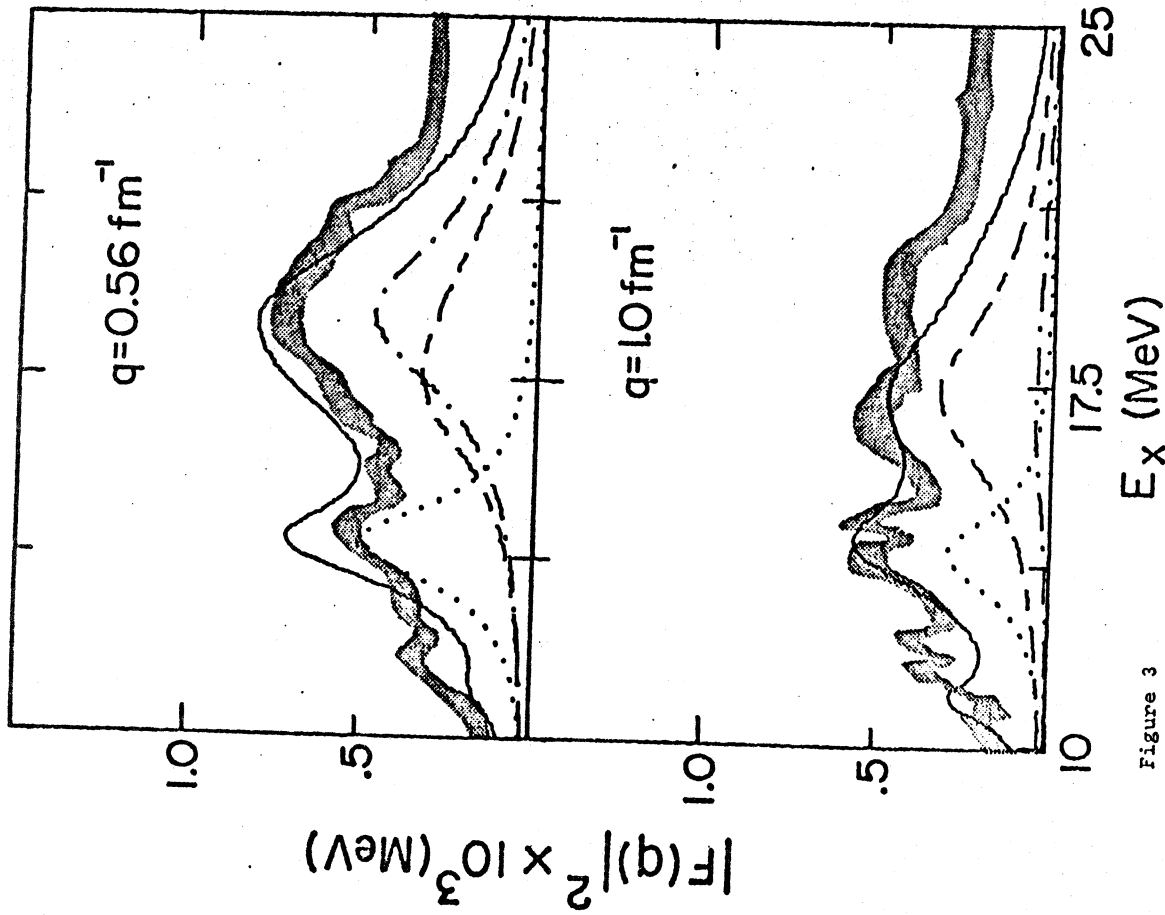
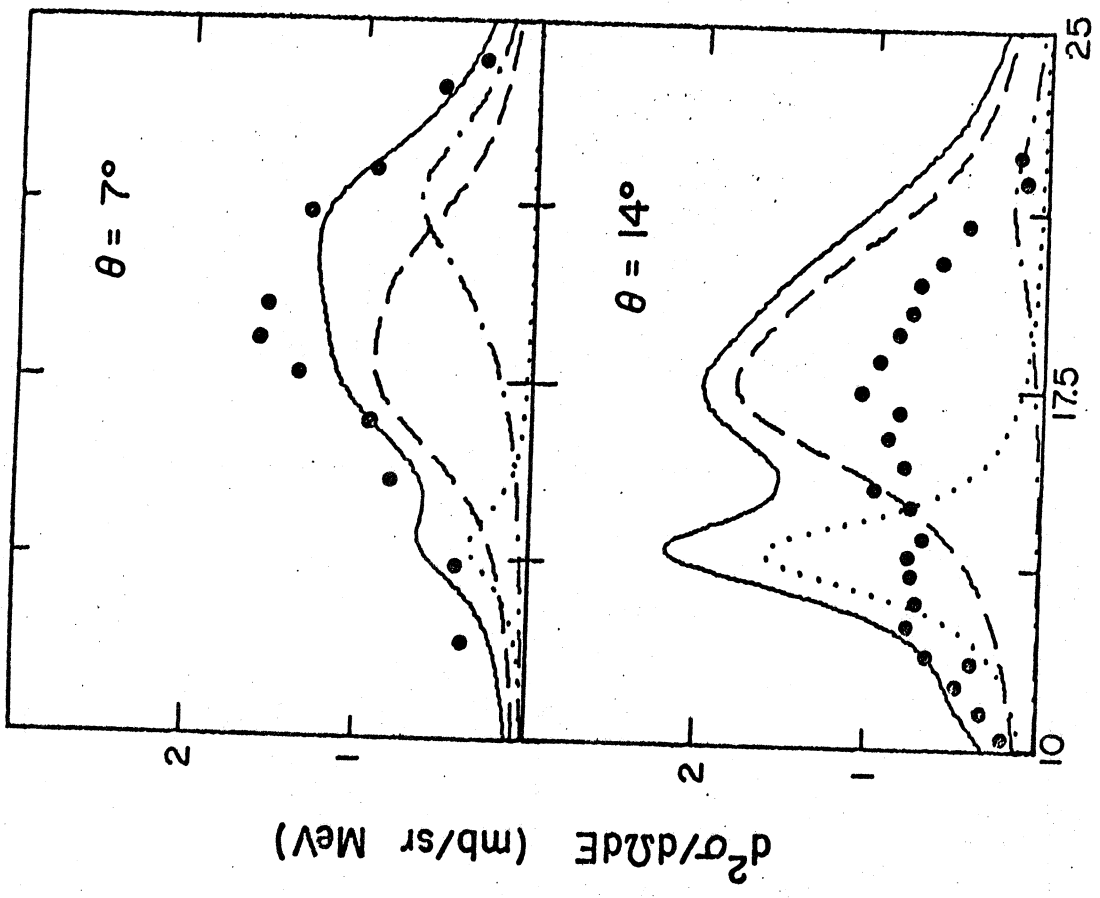


Figure 3

E_x (MeV)

E_x (MeV)

Figure 4



E_x (MeV)

